

# Identification of Candidate Molecular Markers Predicting Sensitivity in Solid Tumors to Dasatinib: Rationale for Patient Selection

Fei Huang,<sup>1</sup> Karen Reeves,<sup>1</sup> Xia Han,<sup>1</sup> Craig Fairchild,<sup>2</sup> Suso Platero,<sup>1</sup> Tai W. Wong,<sup>2</sup> Francis Lee,<sup>2</sup> Peter Shaw,<sup>1</sup> and Edwin Clark<sup>1</sup>

Departments of <sup>1</sup>Clinical Discovery and <sup>2</sup>Oncology Discovery, Bristol-Myers Squibb Co., Princeton, New Jersey

## Abstract

**Dasatinib is a multitargeted kinase inhibitor that was recently approved for the treatment of chronic myelogenous leukemia and Philadelphia chromosome-positive acute lymphoblastic leukemia with resistance or intolerance to prior therapy. It is also in clinical trials for treating patients with solid tumors. The identification of molecular markers predictive of response to dasatinib could assist in clinical development by selecting patients most likely to derive clinical benefit. Using baseline gene expression profiling of a panel of 23 breast cancer cell lines, we identified genomic signatures highly correlated with *in vitro* sensitivity to dasatinib. The ability of these signatures to predict dasatinib sensitivity was further confirmed and validated in independent test cell lines. A six-gene model was used to correctly predict dasatinib sensitivity in 11 out of 12 (92%) additional breast and 19 out of 23 (83%) lung cancer cell lines. Quantitative real-time PCR and immunohistochemical assays further confirmed the differential expression pattern of selected markers. Finally, these gene signatures were observed in a subset of primary breast, lung, and ovarian tumors suggesting potential utility in patient selection. The subset of breast cancer patients expressing the dasatinib-sensitive signature includes a distinct clinical and molecular subgroup: the so-called “triple negative” (i.e., estrogen receptor-negative, progesterone receptor-negative, and HER2-negative) or “basal” breast cancer subtype. This patient population has a poor prognosis and currently has few effective treatment options. Our results implicate that dasatinib may represent a valuable treatment option in this difficult-to-treat population. To test this hypothesis, clinical studies are now under way to determine the activity of dasatinib in these patients. [Cancer Res 2007;67(5):2226–38]**

## Introduction

Utilizing the wealth of information gathered on cancer targets in the so-called “genomics age,” effective targeted therapies have been developed that benefit at least some subsets of patients. Targeting the subset of patients that will benefit should be the developmental goal for such agents. Therefore, new prognostic and predictive molecular markers are needed to accurately predict a patient’s

response to the therapies in development. Such markers would better assess a patient’s sensitivity to a specific therapy, thus facilitating the individualization of therapy. Previous efforts to use genetic information to predict drug sensitivity have primarily focused on individual genes such as *HER2*, *EGFR*, and *UGT* (1–4). More recently, gene expression profiling studies have shown the advantages of genomic “signatures” or marker sets generated by microarray analysis in classifying tumors (5–7), predicting clinical outcome (8, 9), and chemotherapeutic response (10–13). These findings provide hope that cancer treatments of the future will be vastly improved by molecular markers that will enable patient targeting.

Agents targeting novel genes could greatly benefit from such a targeted approach. The SRC tyrosine kinase was the first proto-oncogene described and functions at the hub of a vast array of signal transduction cascades that influence cellular proliferation, differentiation, motility, and survival. SRC has been found to be overexpressed and activated in a large number of cancers, including breast cancer (14), and it has been linked to progression and metastasis in breast cancer (15). Accumulative results suggest SRC as a potential target for designing therapeutics (16, 17), but agents targeting SRC have only been in clinical use since 2003. Dasatinib is a novel, oral, multitargeted kinase inhibitor that targets important oncogenic pathways, including SRC family kinases (SFK) and BCR-ABL (18). In preclinical models, it has shown potent antitumor activity in both *in vitro* cell lines and *in vivo* xenografts (19–23). The results from clinical trials have shown that dasatinib is an effective agent for the treatment of patients with imatinib-refractory chronic myelogenous leukemia and Philadelphia chromosome-positive ALL (24). Dasatinib was recently approved for both indications and is in clinical trials for the treatment of solid tumors.

To support the clinical development of dasatinib, we sought to identify molecular markers predictive of response to this drug that could be used for patient selection during clinical development and beyond. One of challenges is to determine the targeted patient population for the drug before clinical data is available. To overcome this challenge, we generated genomic data in cancer cell lines and correlated it with *in vitro* response to dasatinib to identify candidate markers that may predict response to this therapeutic. We then confirmed and validated the predictive power of the gene signatures in additional cell lines. Finally, we explored the potential utility of the gene signatures in selecting patients likely to respond to dasatinib treatment and identify a target population to be “triple negative” or “basal” breast cancer subtype. Simultaneously and independently, Finn et al. observed that dasatinib preferentially inhibited the growth of basal-type breast cancer cell lines (25). Clinical studies are now under way to determine the activity of dasatinib in these patient populations.

**Note:** Supplementary data for this article are available at Cancer Research Online (<http://cancerres.aacrjournals.org>).

Current address for P. Shaw: Clinical Sciences/Oncology, Merck & Co., Inc., P.O. Box 1000, UG4D72, North Wales, PA 19454.

**Requests for reprints:** Fei Huang, Bristol-Myers Squibb, P.O. Box 5400, HW3B-2.02, Princeton, NJ 08543. Phone: 609-818-5303; Fax: 609-818-5839; E-mail: fei.huang@bms.com.

©2007 American Association for Cancer Research.

doi:10.1158/0008-5472.CAN-06-3633

## Materials and Methods

**Cell culture.** All cell lines were obtained from the American Type Culture Collection (Manassas, VA), except H3396, which was obtained from Pacific Northwest Research Institute (Seattle, WA). The MCF7/Her2 cell line was established by stable transfection of MCF7 cells with the *HER2* gene. Cells were maintained at 37°C under standard cell culture conditions.

**In vitro cytotoxicity assay.** Cells were plated at 4,000 cells per well in 96-well microtiter plates and incubated overnight, then exposed to a serial dilution of dasatinib. After 72 h, cytotoxicity testing was done using MTS assay (26) to determine the sensitivity of cell lines to dasatinib. The results were expressed as an  $IC_{50}$ , which is the drug concentration required to inhibit cell proliferation to 50% of that of untreated control cells. The mean  $IC_{50}$  and SD from multiple tests for each cell line were calculated.

**Gene expression profiling.** RNA was isolated from the cultured cells at ~70% confluence using the RNeasy kits from Qiagen (Valencia, CA). Ten micrograms of total RNA from each cell line was used to prepare biotinylated probe according to the Affymetrix GeneChip Expression Analysis Technical Manual, 2001. Targets were hybridized to Affymetrix high-density oligonucleotide array human HG-U133 set chips (Affymetrix, Santa Clara, CA). The arrays were then washed and stained using the GeneChip Fluidics station according to the instructions of the manufacturer.

**Data analysis.** The expression data on the 23 breast cell lines (training data set; GSE6569) was preprocessed as described in Supplementary Information. The normalized data set was used to select probe sets, the expression level of which correlated with the sensitivity of cells to dasatinib using three statistical methods. First, probe sets were ranked according to their differential expression between sensitive and resistant classes using a signal-to-noise (S2N) metric implemented in the GeneCluster 2.0 software described previously (27, 28). The statistical significance of these gene expression correlations was determined from 1,000 permutation tests to select the top 400 probe sets with  $P < 0.05$ . Second, the Pearson coefficient of correlation  $r$  between the  $IC_{50}$  values of these 23 breast cell lines and the expression level of each probe set was calculated. The probe sets with  $r > 0.4$  or  $r < -0.4$  ( $P < 0.05$ ) were identified and considered as significant. Finally, a Welch  $t$  test was done and the probe sets with  $P < 0.01$  were selected. The probe sets that overlapped between these three statistical methods represent genes significantly correlated with the dasatinib sensitivity/resistance classification.

To further evaluate the predictive ability of the genes identified from the 23 breast cancer cell lines, the expression levels of which are highly correlated with the sensitivity/resistance classification to dasatinib, the weighted-voting algorithm (27, 28) implemented in the GeneCluster 2.0 software was used to predict the sensitivity phenotype of the independent data sets. The complete description of the weighted voting method on how a model is built and how prediction can be made on new cases was described previously (refs. 27, 28; and also available in Supplementary Information).

**Quantitative real-time PCR.** Confirmation of the expression levels of six selected genes identified by microarray analysis was carried out by quantitative real-time PCR (qRT-PCR). cDNA (25 ng) from each sample was amplified with specific primers using the SYBR green Core Reagents kit and a 7900HT real-time PCR instrument (Applied Biosystems, Foster City, CA). The expression of each gene was standardized using glyceraldehyde-3-phosphate dehydrogenase as a reference gene, and relative expression levels for the panel of cell lines were quantified by calculating  $2^{-\Delta\Delta C_T}$ , where  $\Delta\Delta C_T$  is the difference in  $C_T$  between target and reference genes.

**Immunohistochemical assay.** Cells ( $1 \times 10^6$ ) were collected and fixed in 10% formalin for 5 min at room temperature, suspended in agarose, and embedded in paraffin. Five-micrometer tissue sections were cut from each block and placed on positively charged microscope slides. The slides were deparaffinized by immersing in xylene and rehydrated in serial dilutions of 100%, 95%, and 70% ethanol. After rehydration, the slides were washed several times with deionized water at room temperature. Antigen retrieval was done using a BioGenex Citra plus at 95°C for 15 min. The slides were stained in an automated BioGenex i6000 immunohistochemical system.

Both EphA2 and caveolin-1 antibodies were from Santa Cruz Biotechnology (Santa Cruz, CA) and were incubated with slides at 0.5  $\mu\text{g}/\text{mL}$  for 1 h at room temperature followed by three washes in PBS. The envision kit from DAKO (Carpinteria, CA) was used for detection. The slides were then counterstained with hematoxylin for 5 min. As a control, a rabbit IgG was used instead of the primary antibody for the marker being studied. All the negative controls gave no staining (data not shown).

**Western blot analysis.** Cells were either untreated or treated with 0.1  $\mu\text{mol}/\text{L}$  of dasatinib for 1 h. Equal amounts of protein from cell extracts were immunoprecipitated with EPHA2 antibody (Upstate Biotechnology, Lake Placid, NY) and resolved on 10% SDS-polyacrylamide gels. Following transfer to Immobilon-P polyvinyl membrane (Millipore Corp., Bedford, MA), the blots were blocked overnight at 4°C in TBS containing 0.1% Tween 20 detergent and 5% nonfat dry milk. To detect EPHA2, membranes were incubated in the presence of EPHA2 antibody (Upstate Biotechnology). To detect phospho-EPHA2, the same blot was stripped and probed with 0.5  $\mu\text{g}/\text{mL}$  of mouse monoclonal anti-pY20 antibody (BD Biosciences, Lexington, KY). For visualization, chemiluminescence reagent ECL Plus (Amersham Pharmacia Biotech, Piscataway, NJ) was used as directed by the manufacturer.

**Dasatinib treatment of breast cancer cell lines and selection of genes modulated by the drug.** Eleven breast cell lines (MDA-MB-157, MDA-MB-231, HCC1954, HCC70, HCC1806, SK-BR-3, BT-474, MDA-MB-468, HCC1428, ZR-75-1, and MDA-MB-453) with  $IC_{50}$  values ranging from 5.5 nmol/L to 9.5  $\mu\text{mol}/\text{L}$  were treated with 0.4  $\mu\text{mol}/\text{L}$  of dasatinib for 24 h. The expression profiling was done, and a pair-wise comparison between drug-treated and corresponding untreated control was conducted using GeneChip Expression Analysis software MAS 5.0. A change call of “increase” or “decrease” in gene expression level was assigned for each probe set. This analysis was done for all 11 cell lines to compare expression changes upon drug treatment. If a gene was consistently assigned “increase” or “decrease” in at least four cell lines, the gene was considered as modulated by the drug treatment.

**EPHA2 kinase inhibition assay.** An EPHA2 kinase assay was done using 5 to 200 ng of baculovirus-expressed, glutathione affinity-purified EPHA2 fusion protein, 1.5  $\mu\text{mol}/\text{L}$  of poly Glu/Tyr (Sigma, St. Louis, MO), 0.3  $\mu\text{mol}/\text{L}$  of ATP, and 0.15  $\mu\text{Ci}$  [ $\gamma$ - $^{33}\text{P}$ ]ATP in 50  $\mu\text{L}$  kinase buffer [50 mmol/L Tris (pH 7.4), 2 mmol/L DTT, 0.1 mg/mL bovine serum albumin, 0.3 mmol/L  $\text{MnCl}_2$ ]. The reaction mixture was incubated at 28°C for 1 h and the phosphorylated synthetic substrate was quantitated using a TopCount 96-well liquid scintillation counter (Perkin-Elmer Life Sciences, Inc., Boston, MA).

## Results

**The use of breast cancer cell lines to identify candidate predictive markers.** Twenty-three breast cancer cell lines were used to identify candidate markers that may predict response to dasatinib. The sensitivity of these cell lines to dasatinib (i.e., the ability of dasatinib to inhibit cell growth in a proliferation assay, quantified as an  $IC_{50}$  value) ranged from 5.5 nmol/L to >9.5  $\mu\text{mol}/\text{L}$  (Table 1). To classify cell lines as either sensitive or resistant to dasatinib, the mean of the  $\log_{10}(IC_{50})$  across the 23 cell lines was calculated and used as a line of demarcation. The cell lines with  $\log_{10}(IC_{50})$  below the mean were defined as sensitive to the drug, whereas those with  $\log_{10}(IC_{50})$  above the mean were considered to be resistant. As shown in Fig. 1A, 7 and 16 cell lines were classified as either sensitive or resistant to dasatinib, respectively. The sensitive/resistant demarcation was ~0.6  $\mu\text{mol}/\text{L}$  (Table 1). Although the demarcation is arbitrary, data from phase I solid tumor clinical trials showed that 0.6  $\mu\text{mol}/\text{L}$  was within the peak range of dasatinib plasma concentrations in patients treated with the doses near the maximum tolerated dose.

Next, the gene expression profiles for these 23 cell lines were generated. To identify genes correlated with this dasatinib-sensitive/

**Table 1.** Cancer cell lines used in this study with IC<sub>50</sub> to dasatinib, sensitivity classification by IC<sub>50</sub>, and predicted sensitivity by the six-gene predictor

Cell line	IC <sub>50</sub> (μmol/L)	Sensitivity classification based on IC <sub>50</sub>	Sensitivity prediction by six-gene predictor
<b>(A) Training set of breast cancer cell lines</b>			
MDA-MB-157	0.0055	Sensitive	
MDA-MB-231	0.0095	Sensitive	
HCC1954	0.0242	Sensitive	
HCC70	0.0337	Sensitive	
BT-20	0.1652	Sensitive	
HCC1806	0.2194	Sensitive	
HS578T	0.6472	Sensitive	
HCC1419	2.5093	Resistant	
SK-BR-3	2.7534	Resistant	
AU-565	5.2399	Resistant	
HCC38	6.6327	Resistant	
BT-474	6.7375	Resistant	
MDA-MB-468	7.1258	Resistant	
HCC1428	7.2926	Resistant	
MDA-MB-435S	7.7800	Resistant	
H3396	8.1950	Resistant	
BT-549	9.0576	Resistant	
ZR-75-30	9.2632	Resistant	
MCF7	>9.524	Resistant	
MCF7/Her2	>9.524	Resistant	
MDA-MB-436	>9.524	Resistant	
ZR-75-1	>9.524	Resistant	
MDA-MB-453	>9.524	Resistant	
<b>(B) Testing set of breast cancer cell lines</b>			
HCC1143	0.0235	Sensitive	Sensitive
MBA-MB-415	0.0394	Sensitive	Resistant
HCC1937	0.0706	Sensitive	Sensitive
HCC1395	0.0818	Sensitive	Sensitive
UACC-812	1.2158	Resistant	Resistant
MDA-MB-361	1.4383	Resistant	Resistant
HCC1187	1.5793	Resistant	Resistant
DU4475	2.6329	Resistant	Resistant
HCC2157	5.4530	Resistant	Resistant
HCC202	5.5841	Resistant	Resistant
HCC2218	8.6515	Resistant	Resistant
HCC1500	>8.926	Resistant	Resistant
<b>(C) Testing set of lung cancer cell lines</b>			
SK-LU-1	0.0137	Sensitive	Sensitive
L2987	0.0371	Sensitive	Sensitive
H226	0.0583	Sensitive	Sensitive
H838	0.0724	Sensitive	Sensitive
H661	0.1231	Sensitive	Sensitive
NCI-H596	0.1238	Sensitive	Sensitive
H441	0.1411	Sensitive	Sensitive
SK-MES-1	0.1512	Sensitive	Sensitive
H522	0.2151	Sensitive	Resistant
SW1271	0.2424	Sensitive	Sensitive
SW900	0.5074	Sensitive	Sensitive
H2347	1.0246	Resistant	Resistant
H1155	1.0246	Resistant	Resistant
H23	1.0246	Resistant	Sensitive
A-427	>1.025	Resistant	Resistant

**Table 1.** Cancer cell lines used in this study with IC<sub>50</sub> to dasatinib, sensitivity classification by IC<sub>50</sub>, and predicted sensitivity by the six-gene predictor (Cont'd)

Cell line	IC <sub>50</sub> (μmol/L)	Sensitivity classification based on IC <sub>50</sub>	Sensitivity prediction by six-gene predictor
ChaGo-K-1	>1.025	Resistant	Sensitive
A549	>1.025	Resistant	Sensitive
Calu-6	>1.025	Resistant	Resistant
DMS114	>1.025	Resistant	Resistant
DMS53	>1.025	Resistant	Resistant
H157	>1.025	Resistant	Resistant
LX-1	>1.025	Resistant	Resistant
SHP-77	>1.025	Resistant	Resistant

resistant classification, three statistical methods were used (Fig. 1B). By examining the overlap between the genes selected by these three methods (Supplementary Fig. S1), we were able to identify 201 probe sets representing 161 unique genes (28 unique genes have two or more probe sets) that were significantly correlated with the dasatinib sensitivity/resistance classification. As listed in Table 2, there were 83 genes highly expressed in the cell lines sensitive to dasatinib and 78 genes highly expressed in the resistant cell lines. The expression pattern of these genes in the 23 breast cell lines is illustrated in Fig. 1C and a clear separation of sensitive cell lines from a majority of the resistant cell lines was observed (Fig. 1D).

In order to test the ability of the genes listed in Table 2 to discriminate sensitivity to dasatinib in independent test samples, all 161 genes were used to build a predictor based on their expression patterns in the 23 breast cell lines. This predictor was then used to predict the response to dasatinib in 12 additional breast cancer cell lines (Table 1) by using a weighted-voting algorithm (refs. 27, 28; Supplementary Information) implemented in the GeneCluster 2.0 software. The observed sensitive/resistant classification was based on the IC<sub>50</sub> cutoff of 0.6 μmol/L. The 161-gene model correctly predicted three out of four sensitive and all eight resistant breast cancer cell lines, resulting in a sensitivity of 75% and a specificity of 100% (Table 3). A prediction accuracy of 92% (11 of 12) was achieved ( $P = 0.0182$ , Fisher exact test). The positive predictive value and negative predictive value were 100% and 89%, respectively.

**Prioritization of the candidate predictive markers.** Although technologies now exist to examine thousands of genes simultaneously, the identification of a more limited number of markers that predict response to dasatinib might be more useful in clinical studies. Markers were selected based on their biological functions in SFK-related signaling pathways. The Ingenuity Pathways Analysis (Redwood City, CA) tool was initially used to explore the functions and networks of the 161 markers. Gene expression changes or protein modifications caused by inhibiting SRC activity with dasatinib and/or reducing SRC expression with short interfering RNA (siRNA) were further used to help identify genes involved in SFK signaling pathways. To identify genes regulated by dasatinib, 11 breast cancer cell lines were treated with dasatinib. Pair-wise comparisons between cells treated with or without dasatinib were done to identify probe sets that were modulated by the drug treatment. Of the 161 genes which had basal levels that were significantly correlated with sensitivity to dasatinib, 28 were

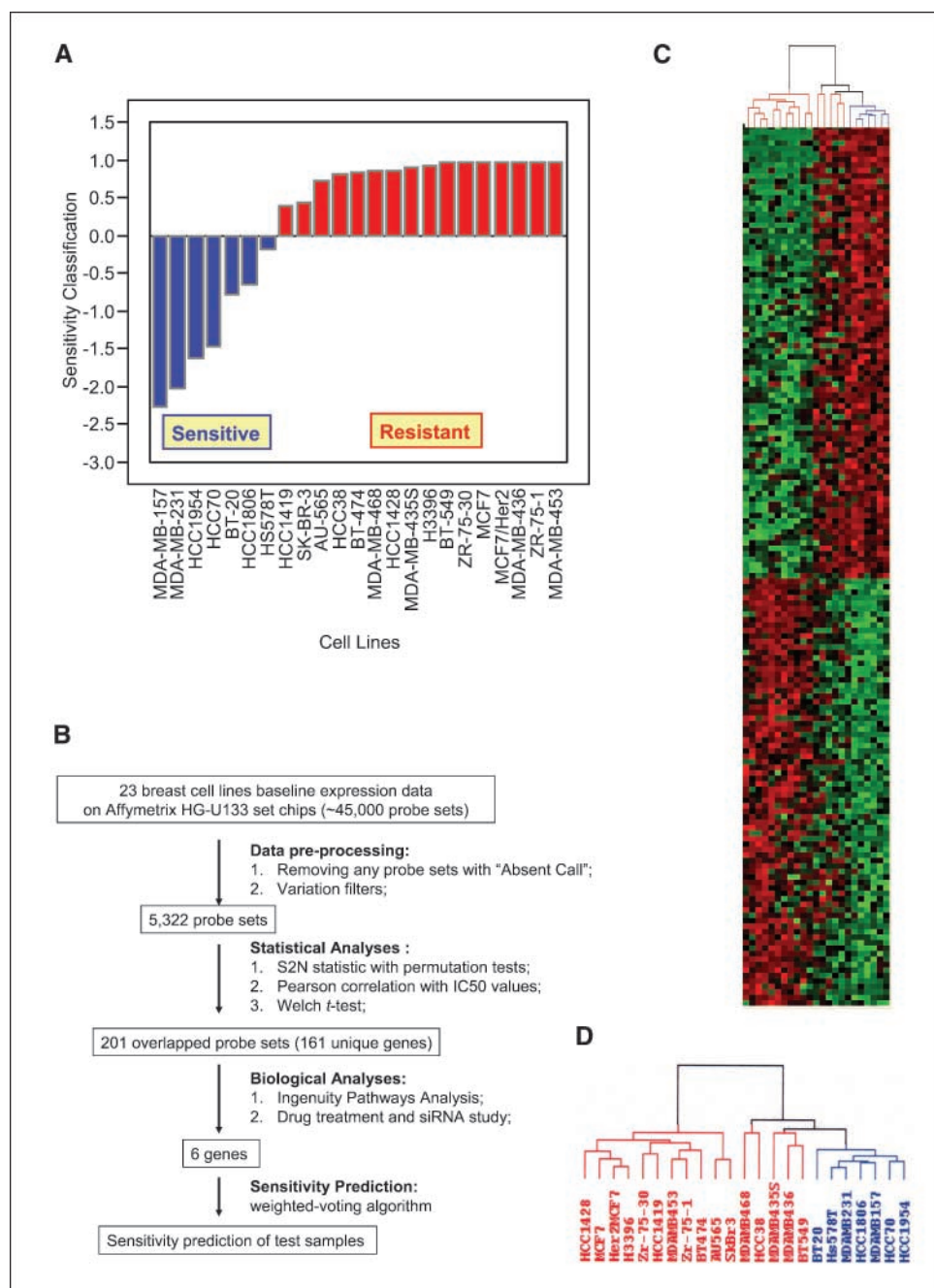
significantly modulated by dasatinib treatment (Table 2). *EPHA2* is shown as an example that the expression level was significantly reduced in response to dasatinib in multiple sensitive breast cancer cell lines (Fig. 2A).

Blocking SRC expression by siRNA was also used to explore whether it has the same effect as dasatinib treatment. Western blot analyses of SRC, *EPHA2*, and *CAVI* was done on SRC-specific siRNA reagent-transfected cells. The results showed that SRC expression was inhibited by an average of 47% in SRC-siRNA-transfected cells (ranging from 24% to 64% for five SRC-siRNA reagents), and *EPHA2* and *CAVI* expression was reduced by 9% to 30% and 13% to 56%, respectively (data not shown). From both dasatinib treatment and SRC-siRNA transfection experiments, it is evident that inhibition of activity or

expression of SRC can down-regulate the expression of both *EPHA2* and *CAVI*.

Because *EPHA2* is a tyrosine kinase and dasatinib is a tyrosine kinase inhibitor, an obvious question is if the down-regulation of *EPHA2* expression by dasatinib is due to a direct effect of the drug on *EPHA2* or through inhibition of SRC activity. SRC-siRNA results suggest that SRC can modulate *EPHA2* expression. However, it is still possible that dasatinib may affect *EPHA2* through two mechanisms: one via SRC inhibition, another through direct inhibition of *EPHA2*. To this end, Western blot analyses was done to evaluate total and phosphorylated *EPHA2* protein levels in nine breast tumor cell lines treated with or without dasatinib. Total *EPHA2* protein levels were not changed after 1 h of dasatinib treatment, whereas the tyrosine phosphorylation of *EPHA2* was

**Figure 1.** Identification of genes correlated with dasatinib sensitivity in the 23 breast cancer cell lines. **A**, the sensitivity/resistance classification of 23 breast cancer cell lines to dasatinib. The classification is based on the mean of  $\log_{10}(IC_{50})$  across the 23 breast cancer cell lines. The cell lines with  $\log_{10}(IC_{50})$  below the mean were defined as sensitive to the drug, whereas those with  $\log_{10}(IC_{50})$  above the mean were considered to be resistant. The sensitive/resistant demarcation was  $\sim 0.6 \mu\text{mol/L}$  in  $IC_{50}$ . **B**, scheme of analysis approaches to identify gene signatures and predictors. **C**, hierarchical clustering analysis showing the relative expression levels of 161 genes that are highly correlated with dasatinib sensitivity/resistance classification of the 23 breast cancer cell lines. *Red*, relatively high expression; *green*, relatively low expression. *Columns*, cell lines; *rows*, genes. The genes are listed in the same order as in Table 2. **D**, sensitive cell lines are separated from the majority of resistant lines in hierarchical clustering analysis. *Blue*, sensitive cell lines; *red*, resistant lines.



Downloaded from http://aacrjournals.org/cancerres/article-pdf/67/15/2229/2867002/2226.pdf by guest on 06 October 2022

**Table 2.** Genes that highly correlated with the sensitivity of 23 breast cancer cell lines to dasatinib

No.	Gene description*	Gene symbol	S2N Score	t test (P)	Correlation with IC <sub>50</sub> <sup>†</sup>	Modulated by dasatinib <sup>‡</sup>
Sensitive gene signature						
1	Jagged 1 (Alagille syndrome)	<i>JAG1</i>	1.67	1.8E-06	-0.59	Decreased
2	Uridine phosphorylase 1	<i>UPPI</i>	1.64	1.6E-04	-0.45	
3	Polymerase I and transcript release factor	<i>PTRF</i>	1.58	4.3E-05	-0.48	Decreased
4	Parvin, $\alpha$	<i>PARVA</i>	1.58	4.8E-06	-0.76	
5	Leprecan-like 1	<i>LEPREL1</i>	1.56	8.0E-05	-0.52	
6	IFN, $\gamma$ -inducible protein 16	<i>IFI16</i>	1.54	6.8E-06	-0.54	Increased
7	Snail homologue 2 (Drosophila)	<i>SNAI2</i>	1.52	2.0E-05	-0.62	
8	Caveolin 2	<i>CAV2</i>	1.47	3.5E-05	-0.48	Decreased
9	Coagulation factor III (thromboplastin, tissue factor)	<i>F3</i>	1.38	3.2E-03	-0.64	
10	Proteasome (prosome, macropain) subunit, $\beta$ type, 8 (large multifunctional protease 7)	<i>PSMB8</i>	1.33	1.0E-04	-0.52	
11	227361_at		1.3	9.9E-03	-0.54	
12	Alkylglycerone phosphate synthase	<i>AGPS</i>	1.3	8.1E-04	-0.55	Decreased
13	Moesin	<i>MSN</i>	1.29	1.3E-04	-0.43	
14	Aldo-keto reductase family 1, member C3 (3- $\alpha$ hydroxysteroid dehydrogenase, type II)	<i>AKRIC3</i>	1.28	4.0E-05	-0.68	Increased
15	tumor necrosis factor receptor superfamily, member 21	<i>TNFRSF21</i>	1.28	5.7E-05	-0.59	
16	Annexin A1	<i>ANXA1</i>	1.24	8.8E-04	-0.40	Decreased
17	Potassium channel tetramerization domain containing 12	<i>KCTD12</i>	1.23	5.1E-03	-0.45	
18	Ras-related C3 botulinum toxin substrate 2 (rho family, small GTP-binding protein Rac2)	<i>RAC2</i>	1.2	6.7E-03	-0.50	
19	Caveolin 1, caveolae protein, 22kDa	<i>CAV1</i>	1.2	4.3E-04	-0.49	Decreased
20	EPH receptor B2	<i>EPHB2</i>	1.19	1.8E-05	-0.61	
21	Nicotinamide N-methyltransferase	<i>NNMT</i>	1.18	4.3E-03	-0.48	Increased
22	La ribonucleoprotein domain family, member 6	<i>LARP6</i>	1.17	1.3E-03	-0.46	
23	Proteasome (prosome, macropain) subunit, $\beta$ type 9 (large multifunctional protease 2)	<i>PSMB9</i>	1.16	1.2E-04	-0.51	
24	Follistatin-like 1	<i>FSTL1</i>	1.14	1.7E-04	-0.49	
25	Anthrax toxin receptor 2	<i>ANTXR2</i>	1.14	3.0E-04	-0.51	
26	Arginine/proline-rich coiled-coil 1	<i>RPRC1</i>	1.13	3.1E-05	-0.51	
27	Exostoses (multiple) 1	<i>EXT1</i>	1.13	7.0E-03	-0.47	
28	Coagulation factor II (thrombin) receptor-like 1	<i>F2RL1</i>	1.12	6.4E-06	-0.62	
29	Inositol polyphosphate-1-phosphatase	<i>INPP1</i>	1.11	2.5E-03	-0.57	
30	Dihydropyrimidine dehydrogenase	<i>DPYD</i>	1.1	2.0E-03	-0.47	
31	FXYD domain containing ion transport regulator 5	<i>FXYD5</i>	1.1	1.8E-05	-0.57	
32	Layilin	<i>LOC143903</i>	1.09	5.0E-03	-0.53	
33	Similar to solute carrier family 16 (monocarboxylic acid transporters), member 14	<i>LOC346887</i>	1.09	2.9E-03	-0.50	
34	Sterile $\alpha$ motif domain containing 9-like	<i>SAMD9L</i>	1.07	1.8E-05	-0.48	
35	Zinc finger protein	<i>ZNF559</i>	1.04	2.1E-05	-0.48	
36	Transforming growth factor, $\beta$ -induced (68 kDa)	<i>TGFBI</i>	1.01	1.7E-03	-0.53	
37	KIAA1949	<i>KIAA1949</i>	1.01	5.4E-03	-0.46	
38	Prion protein (p27-30; Creutzfeld-Jakob disease, Gerstmann-Sträussler-Scheinker syndrome, fatal familial insomnia)	<i>PRNP</i>	1.01	1.3E-03	-0.48	
39	Rho GTPase activating protein 29	<i>ARHGAP29</i>	1	1.6E-03	-0.61	Decreased
40	Oncostatin M receptor	<i>OSMR</i>	0.99	2.1E-04	-0.43	
41	Surfactant-associated protein F mRNA, partial sequence		0.99	7.3E-03	-0.42	
42	Retinoic acid-induced 14	<i>RAI14</i>	0.98	3.3E-03	-0.41	
43	Laminin, $\beta$ 3	<i>LAMB3</i>	0.98	2.3E-03	-0.58	
44	ELK3, ETS domain protein (SRF accessory protein 2)	<i>ELK3</i>	0.98	9.2E-04	-0.47	
45	Suppressor of cytokine signaling 5	<i>SOCS5</i>	0.98	2.0E-03	-0.48	
46	Caldesmon 1	<i>CALD1</i>	0.97	2.9E-03	-0.44	
47	BH-protocadherin (brain-heart)	<i>PCDH7</i>	0.97	2.1E-03	-0.64	
48	Epithelial protein lost in neoplasm $\beta$	<i>EPLIN</i>	0.96	1.2E-03	-0.67	Decreased
49	Popeye domain containing 3	<i>POPC3</i>	0.96	3.0E-03	-0.41	

(Continued on the following page)

**Table 2.** Genes that highly correlated with the sensitivity of 23 breast cancer cell lines to dasatinib (Cont'd)

No.	Gene description*	Gene symbol	S2N Score	t test (P)	Correlation with IC <sub>50</sub> <sup>†</sup>	Modulated by dasatinib <sup>‡</sup>
50	Coactosin-like 1 (Dictyostelium)	<i>COTL1</i>	0.96	6.2E-04	-0.41	Decreased
51	Ubiquitin-conjugating enzyme E2E 3 (UBC4/5 homologue, yeast)	<i>UBE2E3</i>	0.95	1.9E-04	-0.46	
52	Plasminogen activator, urokinase	<i>PLAU</i>	0.94	7.3E-03	-0.49	
53	Epidermal growth factor receptor	<i>EGFR</i>	0.94	1.8E-03	-0.56	Decreased
54	Receptor-interacting serine-threonine kinase 4	<i>RIPK4</i>	0.94	4.2E-03	-0.67	
55	Butyrophilin, subfamily 3, member A3/member A2	<i>BTN3A3/A2</i>	0.93	2.9E-04	-0.59	Increased
56	Tissue factor pathway inhibitor (lipoprotein-associated coagulation inhibitor)	<i>TFPI</i>	0.93	6.4E-03	-0.41	
57	Met proto-oncogene (hepatocyte growth factor receptor)	<i>MET</i>	0.92	2.7E-04	-0.51	Decreased
58	Guanylate-binding protein 3	<i>GBP3</i>	0.92	5.8E-03	-0.49	
59	SH3-domain kinase binding protein 1	<i>SH3KBP1</i>	0.92	7.1E-04	-0.42	
60	Suppression of tumorigenicity 5	<i>ST5</i>	0.92	1.7E-03	-0.50	
61	Interleukin 15 receptor, $\alpha$	<i>IL15RA</i>	0.92	1.4E-03	-0.44	
62	Calpastatin	<i>CAST</i>	0.91	5.6E-04	-0.67	
63	Collagen, type V, $\alpha$ 1	<i>COL5A1</i>	0.9	6.6E-03	-0.43	
64	Kinetochores-associated 2	<i>KNTC2</i>	0.89	1.1E-03	-0.40	
65	Dual-specificity phosphatase 10	<i>DUSP10</i>	0.89	7.1E-04	-0.53	
66	EPH receptor A2	<i>EPHA2</i>	0.89	7.8E-05	-0.58	Decreased
67	Small fragment nuclease	<i>DKFZP566E144</i>	0.89	1.7E-03	-0.51	
68	Butyrophilin, subfamily 3, member A2	<i>BTN3A2</i>	0.89	5.1E-04	-0.52	
69	v-yes-1 Yamaguchi sarcoma viral-related oncogene homologue	<i>LYN</i>	0.88	9.5E-03	-0.42	
70	Myosin X	<i>MYO10</i>	0.88	3.5E-03	-0.54	Decreased
71	Guanine nucleotide-binding protein (G protein), $\gamma$ 12	<i>GNG12</i>	0.85	5.3E-04	-0.50	
72	Discoidin, CUB and LCCL domain containing 2	<i>DCBLD2</i>	0.85	1.2E-04	-0.47	Decreased
73	Mastermind-like 2 (Drosophila)	<i>MAML2</i>	0.85	1.6E-03	-0.47	
74	Transforming growth factor, $\beta$ receptor II (70/80 kDa)	<i>TGFBR2</i>	0.85	6.0E-04	-0.49	
75	Phosphoglucomutase 1	<i>PGM1</i>	0.84	5.6E-03	-0.45	Increased
76	Platelet-derived growth factor C	<i>PDGFC</i>	0.84	1.4E-04	-0.59	Decreased
77	Integrin, $\alpha$ 5 (fibronectin receptor, $\alpha$ -polypeptide)	<i>ITGA5</i>	0.82	3.5E-03	-0.40	
78	Chromosome 3 open reading frame 6	<i>C3orf6</i>	0.82	3.2E-03	-0.42	
79	IFN-induced protein with tetratricopeptide repeats 3	<i>IFIT3</i>	0.82	8.1E-04	-0.45	
80	Elongation factor, RNA polymerase II, 2	<i>ELL2</i>	0.81	1.7E-03	-0.44	
81	PALM2-AKAP2 protein	<i>PALM2-AKAP2</i>	0.81	1.2E-03	-0.48	Decreased
82	CDC42 effector protein (Rho GTPase binding) 3	<i>CDC42EP3</i>	0.81	1.1E-03	-0.61	Decreased
83	Zyxin	<i>ZYX</i>	0.8	1.0E-02	-0.58	
Resistant gene signature						
84	Solute carrier family 1 (glial high affinity glutamate transporter), member 2	<i>SLC1A2</i>	-1.77	1.8E-06	0.64	
85	Chromobox homologue 5 (HP1 $\alpha$ homologue, Drosophila)	<i>CBX5</i>	-1.53	1.5E-04	0.79	
86	239292_at		-1.52	9.3E-05	0.58	
87	Degenerative spermatocyte homologue 2, lipid desaturase (Drosophila)	<i>DEGS2</i>	-1.45	3.7E-05	0.63	
88	Claudin 3	<i>CLDN3</i>	-1.44	1.1E-04	0.52	
89	KIAA0984 protein	<i>KIAA0984</i>	-1.43	2.8E-04	0.42	
90	Phospholipase C, $\beta$ 4	<i>PLCB4</i>	-1.43	6.5E-05	0.55	
91	SH3-binding domain kinase 1	<i>SBK1</i>	-1.43	5.6E-05	0.68	
92	Islet cell autoantigen 1 (69 kDa)	<i>ICA1</i>	-1.4	4.6E-03	0.67	
93	Carbonic anhydrase XII	<i>CA12</i>	-1.33	2.5E-04	0.63	
94	Tumor protein D52	<i>TPD52</i>	-1.32	2.5E-05	0.51	
95	ATP-binding cassette, subfamily A (ABC1), member 3	<i>ABCA3</i>	-1.31	8.8E-06	0.76	
96	KIAA1324	<i>KIAA1324</i>	-1.31	1.1E-04	0.41	
97	DORA reverse strand protein 1	<i>DREV1</i>	-1.23	2.3E-05	0.62	
98	Ret finger protein 2	<i>RFP2</i>	-1.21	8.4E-03	0.60	
99	Solute carrier family 38, member 1	<i>SLC38A1</i>	-1.14	2.2E-03	0.48	

(Continued on the following page)

**Table 2.** Genes that highly correlated with the sensitivity of 23 breast cancer cell lines to dasatinib (Cont'd)

No.	Gene description*	Gene symbol	S2N Score	t test (P)	Correlation with IC <sub>50</sub> <sup>†</sup>	Modulated by dasatinib <sup>‡</sup>
100	Cyclic AMP-responsive element binding protein 3-like 4	<i>CREB3L4</i>	-1.14	3.4E-03	0.42	
101	Chromosome 17 open reading frame 28	<i>C17orf28</i>	-1.14	7.6E-03	0.41	
102	Cisplatin resistance-associated overexpressed protein	<i>CROP</i>	-1.11	4.2E-03	0.61	
103	Phospholipase C-like 3	<i>PLCL3</i>	-1.11	6.2E-04	0.42	
104	Abhydrolase domain containing 11	<i>ABHD11</i>	-1.09	9.2E-04	0.54	
105	230085_at		-1.09	5.2E-05	0.57	
106	Arg/Abl-interacting protein ArgBP2	<i>ARGBP2</i>	-1.08	4.4E-03	0.54	
107	Solute carrier family 35 (CMP-sialic acid transporter), member A1	<i>SLC35A1</i>	-1.08	1.1E-04	0.64	
108	Solute carrier family 16 (monocarboxylic acid transporters), member 6	<i>SLC16A6</i>	-1.03	1.5E-03	0.51	
109	FLJ21963 protein	<i>FLJ21963</i>	-1.02	7.4E-04	0.41	
110	ATP-binding cassette, subfamily G (WHITE), member 1	<i>ABCG1</i>	-1.02	9.7E-04	0.49	
111	Cytochrome b-561	<i>CYB561</i>	-1.02	3.1E-03	0.44	
112	Achaete-scute complex-like 2 (Drosophila)	<i>ASCL2</i>	-1.02	1.2E-04	0.50	
113	Insulin-like growth factor binding protein 2 (36 kDa)	<i>IGFBP2</i>	-1.01	9.9E-03	0.53	
114	Prolactin receptor	<i>PRLR</i>	-1.01	1.7E-03	0.44	
115	Glycerol-3-phosphate dehydrogenase 1-like	<i>GPDL1</i>	-1.01	6.4E-04	0.41	
116	Junctophilin 1	<i>JPH1</i>	-1	7.3E-05	0.43	
117	Epidermal growth factor receptor pathway substrate 15-like 1	<i>EPS15L1</i>	-0.99	1.8E-03	0.67	
118	Programmed cell death 4 (neoplastic transformation inhibitor)	<i>PDCD4</i>	-0.98	7.2E-04	0.50	Increased
119	Microtubule-associated protein $\tau$	<i>MAPT</i>	-0.98	2.5E-04	0.65	
120	Chromosome 14 open reading frame 83	<i>C14orf83</i>	-0.97	4.2E-04	0.54	
121	Isochorismatase domain containing 1	<i>ISOC1</i>	-0.96	1.0E-03	0.46	
122	Aristaless-related homeobox	<i>ARX</i>	-0.95	3.7E-04	0.50	
123	Trichorhinophalangeal syndrome 1	<i>TRPS1</i>	-0.95	1.8E-04	0.55	
124	239847_at		-0.95	1.6E-03	0.43	
125	Vacuolar protein sorting 37C (yeast)	<i>VPS37C</i>	-0.95	5.1E-03	0.56	
126	LAG1 longevity assurance homologue 6 ( <i>S. cerevisiae</i> )	<i>LASS6</i>	-0.94	1.2E-03	0.47	
127	Scavenger receptor class B, member 1	<i>SCARB1</i>	-0.94	6.6E-03	0.42	
128	Phosphatidylinositol 3,4,5-trisphosphate-dependent RAC exchanger 1	<i>PREX1</i>	-0.94	2.0E-03	0.46	
129	225996_at		-0.94	2.0E-03	0.49	
130	Cholinergic receptor, muscarinic 1	<i>CHRM1</i>	-0.94	9.5E-05	0.52	
131	GREB1 protein	<i>GREB1</i>	-0.93	1.5E-03	0.55	
132	Choline phosphotransferase 1	<i>CHPT1</i>	-0.92	3.4E-04	0.72	
133	Eukaryotic translation initiation factor 4E member 3	<i>EIF4E3</i>	-0.91	7.4E-03	0.58	
134	Ubiquitin-like 3	<i>UBL3</i>	-0.91	7.4E-03	0.52	
135	Spinster	<i>SPIN1</i>	-0.9	5.2E-03	0.62	
136	Calmodulin 1 (phosphorylase kinase, $\delta$ )	<i>CALM1</i>	-0.9	3.9E-03	0.48	
137	Hypothetical LOC131076	<i>LOC131076</i>	-0.9	9.3E-03	0.54	
138	Phosphoinositide-3-kinase-related kinase SMG-1-like	<i>DKFZp547E087</i>	-0.9	1.4E-03	0.52	
139	Myelin expression factor 2	<i>MYEF2</i>	-0.9	7.9E-03	0.59	
140	Solute carrier family 25 (mitochondrial carrier; ornithine transporter) member 15	<i>SLC25A15</i>	-0.89	6.1E-03	0.62	
141	Chromosome 6 open reading frame 108	<i>C6orf108</i>	-0.88	1.0E-03	0.67	
142	YME1-like 1 ( <i>S. cerevisiae</i> )	<i>YME1L1</i>	-0.87	2.1E-03	0.50	
143	Williams-Beuren syndrome, critical region protein 20 copy B	<i>WBSCR20B</i>	-0.86	1.2E-03	0.59	
144	239065_at		-0.85	9.4E-03	0.52	
145	Acyl-CoA synthetase long-chain family member 3	<i>ACSL3</i>	-0.84	8.2E-03	0.58	
146	230991_at		-0.84	2.9E-03	0.43	
147	Trefoil factor 1 (breast cancer, estrogen-inducible sequence expressed in)	<i>TFF1</i>	-0.84	6.2E-04	0.45	Increased
148	Epithelial membrane protein 2	<i>EMP2</i>	-0.84	1.0E-02	0.47	
149	Chromosome 14 open reading frame 93	<i>C14orf93</i>	-0.83	5.1E-04	0.52	

(Continued on the following page)

**Table 2.** Genes that highly correlated with the sensitivity of 23 breast cancer cell lines to dasatinib (Cont'd)

No.	Gene description*	Gene symbol	S2N Score	t test (P)	Correlation with IC <sub>50</sub> <sup>†</sup>	Modulated by dasatinib <sup>‡</sup>
150	START domain containing 10	<i>STARD10</i>	-0.83	8.9E-04	0.43	Increased
151	Ceroid-lipofuscinosis, neuronal 3, juvenile (Batten, Spielmeyer-Vogt disease)	<i>CLN3</i>	-0.83	1.6E-03	0.49	
152	Ras homologue gene family, member B	<i>RHOB</i>	-0.82	3.1E-03	0.42	Increased
153	Erythrocyte membrane protein band 4.1-like 5	<i>EPB41L5</i>	-0.81	7.8E-03	0.41	
154	Iroquois homeobox protein 5	<i>IRX5</i>	-0.8	1.0E-02	0.51	
155	Hypothetical protein LOC92482	<i>LOC92482</i>	-0.8	8.2E-03	0.48	Increased
156	CDC42 small effector 1	<i>CDC42SE1</i>	-0.8	1.0E-02	0.50	
157	Pleckstrin homology domain containing, family H (with MyTH4 domain) member 1	<i>PLEKHH1</i>	-0.79	7.5E-05	0.56	
158	EGF-like domain, multiple 5	<i>EGFL5</i>	-0.79	1.0E-02	0.52	
159	239319_at		-0.78	1.5E-03	0.42	
160	Transducer of ERBB2, 1	<i>TOB1</i>	-0.78	3.9E-03	0.42	Increased
161	Crn, crooked neck-like 1 (Drosophila)	<i>CRNKL1</i>	-0.77	1.5E-03	0.44	

NOTE: Sensitive and resistant gene signatures are listed separately and ranked by S2N score. Positive or negative signs correspond to genes being more highly expressed in sensitive class or resistant class.

\*For nonannotated genes, Affymetrix probe set ID are provided as the identification.

<sup>†</sup> Correlation between the IC<sub>50</sub> values and the expression level of each gene in cell lines was assessed by Pearson correlation coefficient *r*.

<sup>‡</sup> Eleven breast cell lines were treated with 0.1 μmol/L of dasatinib for 24 h. Pair-wise comparisons between cells treated with or without dasatinib were done, genes whose expressions were significantly increased or decreased in at least four cell lines were considered to be modulated by the drug treatment.

dramatically decreased (Fig. 2B). This led us to further test whether dasatinib can directly inhibit EPHA2 kinase activity. *In vitro* kinase inhibition assays were done. The results showed that dasatinib has an IC<sub>50</sub> of 17 nmol/L for EPHA2, higher than for SFKs and BCR-ABL (0.2–3 nmol/L) as described by Lombardo et al. (18), but still likely to be important physiologically.

**Assessment of the accuracy of a six-gene model in predicting sensitivity to dasatinib.** Although markers with high statistical significance are candidates in building a predictive model, markers

with both statistical significance and biological relevance to the targeted pathway may be even more useful in building predictive models. Among the genes that are correlated with sensitivity to dasatinib and modulated upon treatment with dasatinib and/or SRC-siRNA, six genes (*EPHA2*, *CAV1*, *CAV2*, *ANXA1*, *PTRF*, and *IGFBP2*) were selected for further assessment. All six of these genes are either targets of dasatinib, are substrates for SRC family kinases, or are part of signaling pathways downstream of SRC family kinases. First, these six genes were used to build a predictor

**Table 3.** Dasatinib sensitivity prediction of testing cell lines using the 161-gene and 6-gene predictors

Observed/predicted	Sensitive (no.)	Resistant (no.)	Total (no.)	Correct prediction (%)
One hundred and sixty-one-gene predictor				
Twelve breast cancer cell lines				
Sensitive	3	1	4	75
Resistant	0	8	8	100
Total	3	9	12	
Twenty-three lung cancer cell lines				
Sensitive	7	4	11	64
Resistant	2	10	12	83
Total	9	14	23	
Six-gene predictor				
Twelve breast cancer cell lines				
Sensitive	3	1	4	75
Resistant	0	8	8	100
Total	3	9	12	
Twenty-three lung cancer cell lines				
Sensitive	10	1	11	91
Resistant	3	9	12	75
Total	13	10	23	



based on the expression results of the 23 breast cancer cell lines that were initially used to select candidate genes. Second, the predictive power of the six-gene predictor was tested on the test set of 12 breast cancer cell lines. The same prediction result was obtained using the 6-gene predictor as using the 161-gene predictor (Table 3). Because the value of a predictor that could be used across indications is greater than one that works in a single indication, we tested the accuracy of both the 6-gene and the 161-gene models in another test set of 23 lung cancer cell lines (Table 1). As shown in Table 3, the prediction accuracy for the 6-gene predictor and the 161-gene predictor was 83% (19 of 23) and 74% (17 of 23), respectively, suggesting that the 6-gene predictor might be more useful in additional indications.

The prediction power of the six-gene predictor was further assessed in seven tumor xenografts that were generated either from cancer cell lines (breast, MCF-7; prostate, PC3 and MDAPCa-2b; and colon, WiDr) or from pancreatic tumors (Pat-25, Pat-26, and Pat-27). Xenografts Pat 26, Pat27, PC3, and WiDr were predicted to be sensitive, whereas Pat 25, MCF-7, and MDAPCa-2b were predicted to be resistant to dasatinib; the predicted result matched perfectly with *in vivo* antitumor activity for these xenografts (data not shown).

The expression level of these six genes was further confirmed using qRT-PCR. The correlation between the expression values obtained by Affymetrix microarray analysis and by qRT-PCR for each gene in the panel of 23 breast cell lines was measured by Pearson correlation coefficient  $r$ , which was determined to be 0.90, 0.94, 0.93, 0.82, 0.94, and 0.98 for *EPHA2*, *CAVI*, *CAV2*, *ANXA1*, *PTRF*, and *IGFBP2*, respectively. The results indicated statistically good correlations ( $P < 0.001$  for all six genes) obtained by these two analysis methods. The fold change in the average expression values between 7 sensitive and 16 resistant cell lines detected by both technologies showed a high correlation for these six genes (Fig. 3A).

To determine if the protein levels for these candidate genes were correlated with mRNA expression levels, immunohistochemical assays were developed to evaluate the protein expression of EPHA2 and CAV1. Three breast cancer cell lines (MDA-MB-231, BT-474, and MCF7) were selected for immunohistochemical testing and as illustrated in Fig. 3B, the highest expression was observed in the sensitive MDA-MB-231 cell line, whereas lower expression was observed in the resistant cell lines BT-474 and MCF7. The immunohistochemical results were consistent with the results obtained from RNA expression as measured by both microarray and qRT-PCR. Moreover, the results showed that the protein levels of these two genes were also correlated with the sensitivity of cell lines to dasatinib, suggesting that both RNA- and protein-based assays may have utility in predicting response to dasatinib.

**Gene signatures and predicting response to dasatinib in multiple tumor types.** To explore whether the 161-gene signature also exists in primary breast tumors, an expression data set of 134 primary breast tumor specimens (29) was examined. Hierarchical clustering analysis (Supplementary Fig. S2A) classified the breast tumors into two distinct groups with one group of tumors (red cluster) expressing the gene signature found in dasatinib-resistant cell lines and the other group (blue cluster) expressing the gene signature found in dasatinib-sensitive cell lines. A similar pattern was also observed for lung (Supplementary Fig. S2B) and ovarian tumors (data not shown). Our next goal was to estimate the percentage of cancer patients predicted to be responsive to dasatinib using the six-gene predictor identified by *in vitro* breast

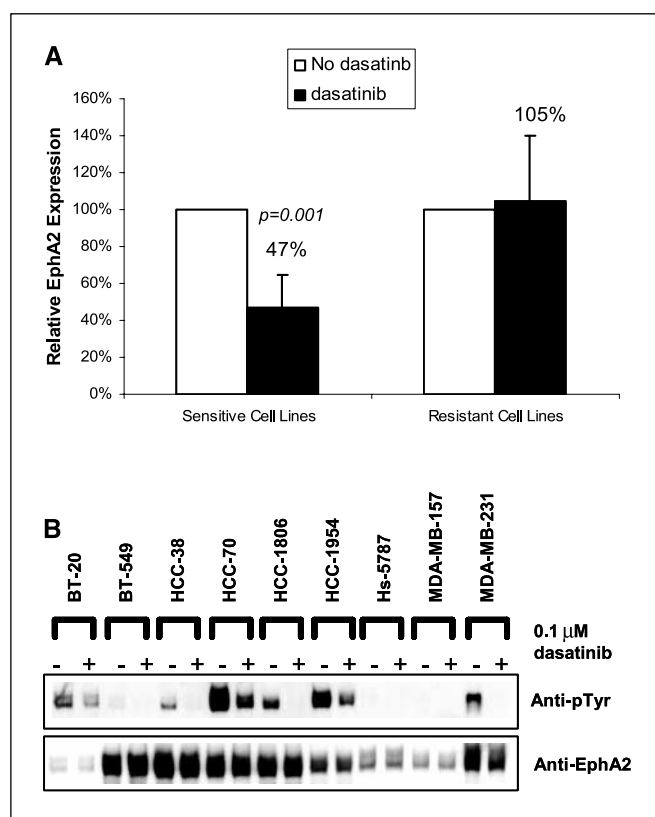


**Figure 2.** Gene expression level and tyrosine phosphorylation status of Epha2 changed upon dasatinib treatment in multiple breast cancer cell lines. **A**, EPHA2 gene expression levels decreased in response to dasatinib in sensitive breast cell lines measured by qRT-PCR. The values (%) are results to compare the 24-h dasatinib-treated cell line to the corresponding untreated control and represented as mean  $\pm$  SE of five sensitive cell lines (MDA-MB-157, MDA-MB-231, HCC1954, HCC70, and HCC1806) or six resistant cell lines (SK-BR-3, BT-474, MDA-MB-468, HCC1428, ZR-75-1, and MDA-MB-453). **B**, Western blot analysis of EPHA2 protein level and tyrosine phosphorylation status in nine breast cancer cell lines. Cells were treated with or without 0.1  $\mu$ mol/L of BMS-354825 for 1 h. Cell lysates were immunoprecipitated with Epha2 antibody and analyzed by p-Tyr and Epha2 immunoblots.

cancer cell lines. Gene expression databases for breast, lung, and ovarian cancer were interrogated. Depending on the tumor type, 30% to 40% of the patients were predicted to be responsive to dasatinib (Table 4).

To further investigate the dasatinib-responsive subpopulation predicted by the six-gene model in breast cancer, we examined several well-known markers that define breast cancer subtypes. The expression level of ER, PR, and HER2 was assessed for the dasatinib-responsive and nonresponsive subpopulations. Most strikingly, as shown in Table 5, there were significant differences in the distribution of tumors expressing ER, PR and/or HER2 between the two groups (e.g., a higher percentage of the patients predicted to be dasatinib-responsive were ER/PR/HER2-negative). Furthermore, a higher percentage of tumors with high expression levels of KRT5 and KRT17 were observed in the patients predicted to be responders compared with those predicted to be non-responders, suggesting dasatinib responding tumors may include the basal type of breast cancer as defined by KRT5/KRT17 expression (30). This analysis was also done using the 161-gene signatures and similar results (Supplementary Fig. S2C and D) were observed between the dasatinib-responder (blue cluster) and nonresponder (red cluster) groups.

## Discussion

This study focused on the identification of a molecular signature that could be used to guide early clinical development of dasatinib in solid tumors. We conducted preclinical pharmacogenomic studies in a panel of cancer cell lines to identify 161 genes, the expression levels of which were significantly correlated with the sensitivity/resistance classification to dasatinib. The RNA and protein expression levels of selected genes were further confirmed and validated by qRT-PCR and immunohistochemical assays. Finally, predictive models built with the 161 genes and with a smaller set of 6 genes were independently validated on both breast and lung cancer cell lines.

Many of the 161 genes identified in this study are linked to signaling pathways of SFKs, including genes involved in cell cycle, cell growth and proliferation, apoptosis, adhesion and migration. The expression of LYN, a SFK member (31), is correlated with sensitivity to dasatinib in breast cancer cell lines (Table 2), even though SRC expression is not. Genes such as *CAV1* and *CAV2* that are highly expressed in dasatinib sensitive cell lines are substrates for SFKs and functionally involved in SFK signaling pathways (32). Furthermore, it has been suggested that CAV1 protein is necessary for the activation of SFKs which then induce the tyrosine phosphorylation of focal adhesion kinase (33, 34). Many genes

down-regulated by dasatinib treatment are involved in functions that SFKs have been previously implicated, suggesting an important role for dasatinib in modulating SFK signaling.

SFKs are intracellular membrane-associated tyrosine kinases that are required for mitogenesis initiated by multiple growth factor receptors, including the epidermal growth factor receptor (EGFR), platelet-derived growth factor receptor, hepatocyte growth factor receptor (Met), fibroblast growth factor receptor, and colony-stimulating factor receptor through growth factor ligand binding (35). It has been reported that in highly metastatic human colon cancer cell lines, both MET and EGFR activate SRC (36). In some human breast cancers there is evidence that synergism between SFKs and EGFR or Met may contribute to tumor growth (37). Our results show that expression of several receptor tyrosine kinase (e.g., EPHA2, EPHB2, EGFR and MET) are correlated with sensitivity to dasatinib, suggesting that combination treatment of dasatinib with inhibitors of EGFR and/or MET may represent an attractive approach for treatment of patients with tumors expressing these kinases. EPHA2 and EPHB2 are members of the largest family of tyrosine kinase receptors. EPHA2, is highly expressed in many human cancers and often associated with poor prognostic features and it is involved in many processes crucial to

**Figure 3.** Differential expression levels of candidate markers measured by Affymetrix GeneChip, qRT-PCR, and immunohistochemistry. **A**, comparison of fold change in the expression levels of six genes between 7 sensitive and 16 resistant breast cancer cell lines detected by Affymetrix GeneChip and qRT-PCR. **B**, protein expression of EPHA2 and CAV1 assessed by immunohistochemistry in three breast cancer cell lines (magnification,  $\times 40$ ). Positive staining is indicated by the presence of a brown chromagen. As a negative control, a rabbit IgG was used and all the negative controls gave no staining (data not shown). Higher levels of both EPHA2 and CAV1 are detected in dasatinib-sensitive cell line MDA-MB-231 and lower levels are detected in dasatinib-resistant cell lines BT-474 and MCF7.

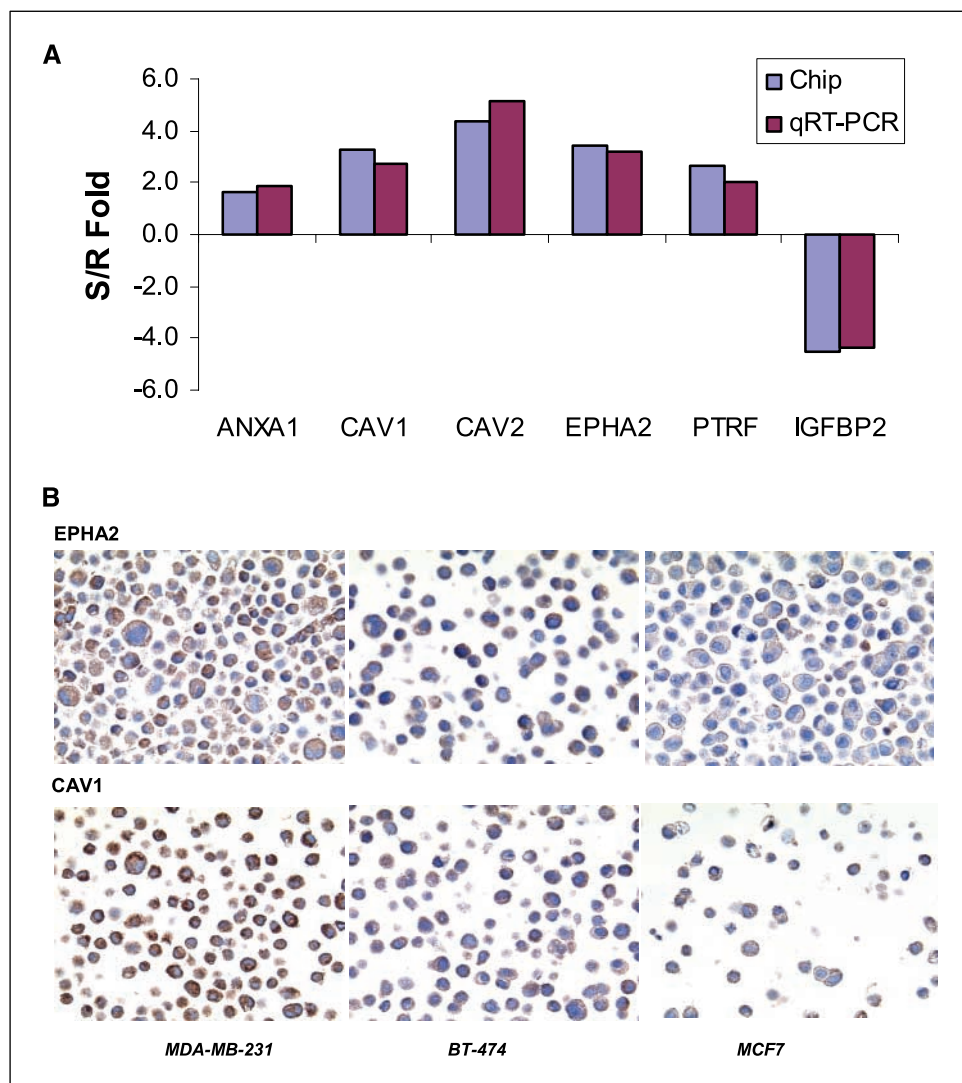


**Table 4.** Dasatinib response prediction of different tumor samples using the six-gene predictor

Tumor type	Total number	Predicted "dasatinib-sensitive", no. (%)	Data set source
Breast	184	65 (35)	GSE2109
Breast	134	54 (40)	Internal
Lung	64	25 (40)	GSE2109
Lung	29	12 (41)	Internal
Ovary	93	32 (34)	GSE2109
Ovary	146	47 (32)	GSE3149

malignant progression, such as migration, invasion, metastasis, proliferation, survival and angiogenesis (38). Our results show that EPHA2 is highly expressed in dasatinib sensitive cell lines and its expression, phosphorylation and kinase activity are reduced upon dasatinib treatment, indicating that EPHA2 is one of the downstream targets for dasatinib.

Although SRC expression is not correlated with the sensitivity of breast cancer cell lines to dasatinib, the activation status of the SRC pathway may be. A recent report identified a gene expression signature that reflects the activation status of the SRC oncogenic pathway, and the signature can predict the sensitivity of a broad range of human tumor cell lines to a SRC inhibitor, SU6656 (39). When we use the SRC pathway signature to perform clustering analysis on the 23 breast cell lines, an expression pattern similar to the one shown in Fig. 1D was observed (Supplementary Fig. S3) with dasatinib sensitive cell lines separated from resistant ones, further confirming the finding that cancer cell lines with an activated oncogenic pathway can be correlated with sensitivity to therapeutic agents that target components of that pathway. The results show that different analytic approaches to identify markers of sensitivity to agents targeting specific oncogene may identify the same subset of cell lines and, ultimately, patients that will benefit from such agents.

The selection of 6 genes from the initial set of 161 genes to build a predictive model was based on their biological functions in SRC family kinase-related signaling pathways and availability for assay development. This selection is empirical and alternative predictors consisting of different combinations of genes from the 161 genes

may be equally predictive as the 6-gene model identified herein. As recently discussed by Fan et al. (40) although different gene sets are being used for prognostication in patients with breast cancer, they each track a common set of biological characteristics and result in similar predictions of outcome. The observation that the 161-gene signature and the SRC pathway signature (39) identify a similar set of breast cell lines as either sensitive or resistant to SFK inhibitors such as dasatinib supports the observation by Fan et al. (Fig. 1D; Supplementary Fig. S3).

Interestingly, a simultaneous and independent study by Finn et al. using a different array platform (Agilent), different cell lines, and different assays for proliferation identified three genes *CAVI*, *MSN* and *YAPI* to be highly expressed in dasatinib sensitive breast cell lines and predictive of dasatinib sensitivity (25). Both *CAVI* and *MSN* were identified in our study, and *YAPI* just missed our stringent statistical cutoff ( $t$  test  $P = 0.025$  in our study).

A number of genes in Table 2 were reported to be associated with sensitivity or resistance to other anticancer agents. A study of the molecular markers associated with four anticancer platinum compounds (cisplatin, carboplatin, tetraplatin and oxaliplatin) in cancer cell lines indicated that the expression level of *CAV2* and *F3* are correlated with sensitivity to both tetraplatin and oxaliplatin, whereas *CAVI*, *TGFBR2* and *CALD1* only correlated with sensitivity to oxaliplatin (41). Another gene, *MYO10* is elevated in both oxaliplatin and carboplatin chemosensitive cells (41, 42). All these genes are also expressed at higher levels in dasatinib sensitive cell lines (Table 2). On the other hand, genes that had expressions which were elevated in dasatinib-resistant cell lines included *IGFBP2*, *IRX5*, and *MAPT*, each of which have been reported to be associated with chemoresistance to the platinum drug AMD473 (43), to 5-fluorouracil (44), and to paclitaxel (45), respectively. *EMP2* is another resistant marker for dasatinib, whereas *EMPI* was identified as both a *de novo* and acquired marker of gefitinib resistance (46). Multidrug resistance of tumors is frequently associated with decreased cellular accumulation of anticancer drugs and elevated expression of ATP-binding cassette (ABC) transporters. Although, dasatinib is not a substrate of MDRI, other ABC transporter genes such as *ABCA3* and *ABCG1* were highly expressed in dasatinib resistant cell lines, suggesting they may contribute to the resistance mechanism of dasatinib. Additional experiments will be needed to address the role of each marker that contributes to the complex phenotype associated with drug sensitivity and resistance.

**Table 5.** Distribution of "high" and "low" expresser of ER, PR, HER2, and KRT5/17 between dasatinib-responder and nonresponder breast tumor groups predicted by the six-gene predictor

Gene	Expression level*	Predicted nonresponder (80)	Predicted responder (54)	$\chi^2$ test ( $P$ )
<i>HER2</i>	H	46	21	0.035
	L	34	33	
<i>ER</i>	H	47	20	0.014
	L	33	34	
<i>PR</i>	H	45	22	0.078
	L	35	32	
<i>KRT 5/17</i>	H	28	31	0.010
	L	52	23	

\*The median expression level of a gene across the 134 tumors was used to define "high" (H) or "low" (L) expression. A tumor was designated as "L" if its expression was below the median level and designated as "H" if its expression was above the median.

The results in this study clearly showed that the six-gene predictor identified from the 23 breast cell lines can be used to predict the sensitivity to dasatinib not only in breast but also in lung cancer cell lines (prediction accuracy of 92% and 83%, respectively, in independent test sets). We have used the six-gene predictor to identify 30% to 40% of primary breast, lung and ovarian cancer patients for whom dasatinib might be beneficial. For breast tumors, the expression status of ER, PR and HER2 was examined and found to correlate with dasatinib sensitivity, allowing us to recognize a patient subpopulation that can be identified using diagnostics currently available to oncologists. The predicted dasatinib-responsive subgroup tends to have more tumors with lower expression of ER, PR, or HER2 gene and more tumors with higher expression of KRT5/KRT17 (Table 5; Supplementary Fig. S2C and D). An independent study supported our observations by showing that the majority of dasatinib-sensitive breast cancer cell lines were "basal" type or "triple-negative" (25). This patient population is one that currently does not benefit from conventional targeted therapies such as endocrine therapy or trastuzumab, leaving only chemotherapy in the therapeutic armamentarium. Considering that these patients express a dasatinib-sensitive gene signature, this drug may represent a valuable treatment option in this difficult-to-treat population of patients with breast cancer and clinical studies are now under way to determine the activity of dasatinib in these patients.

The clinical utility of such a predictor will now be tested in clinical studies. It should be noted that dasatinib is, *in vitro*, a cytostatic agent that is more likely to have an effect on disease control than to cause tumor regressions. Furthermore, our efforts have focused on identifying markers that will predict those tumors for which dasatinib will have an antiproliferative effect. It is possible that dasatinib will also show benefit in cancer patients that do not have the predictive signature identified in this study for two reasons. First, because SRC plays an important role downstream of vascular endothelial growth factor signaling (47, 48), it is likely that dasatinib will also have antiangiogenic effects. Second, because SRC plays an important role in osteoclast function (49), it is possible that dasatinib will benefit patients with bone metastases. The role of dasatinib as an antiangiogenic and anti-bone metastases agent will be explored in separate clinical studies.

## Acknowledgments

Received 9/29/2006; revised 11/2/2006; accepted 12/13/2006.

The costs of publication of this article were defrayed in part by the payment of page charges. This article must therefore be hereby marked *advertisement* in accordance with 18 U.S.C. Section 1734 solely to indicate this fact.

We thank Russell Peterson, Kathy Johnston, Qiuyan Wu, Nancy Perkins, David Kan, Ivan Inigo, and Stephen Castenada for technique support, and Drs. Jonas Bergh, Judith Bjöhle, and Suzanne Egyhazi from Karolinska Institute for providing the breast tumor RNA samples.

## References

- Baselga J, Tripathy D, Mendelsohn J, et al. Phase II study of weekly intravenous recombinant humanized anti-p185HER2 monoclonal antibody in patients with HER2/neu-overexpressing metastatic breast cancer. *J Clin Oncol* 1996;14:737-44.
- Lynch TJ, Bell DW, Sordella R, et al. Activating mutations in the epidermal growth factor receptor underlying responsiveness of non-small-cell lung cancer to gefitinib. *N Engl J Med* 2004;350:2129-39.
- Pao W, Miller V, Zakowski M, et al. EGF receptor gene mutations are common in lung cancers from "never smokers" and are associated with sensitivity of tumors to gefitinib and erlotinib. *Proc Natl Acad Sci U S A* 2004;101:13306-11.
- Carlini LE, Meropol NJ, Bever J, et al. UGT1A7 and UGT1A9 polymorphisms predict response and toxicity in colorectal cancer patients treated with capecitabine/irinotecan. *Clin Cancer Res* 2005;11:1226-36.
- Perou CM, Sorlie T, Eisen MB, et al. Molecular portraits of human breast tumours. *Nature* 2000;406:747-52.
- Sorlie T, Perou CM, Tibshirani R, et al. Gene expression patterns of breast carcinomas distinguish tumor subclasses with clinical implications. *Proc Natl Acad Sci U S A* 2001;98:10869-74.
- Brenton JD, Carey LA, Ahmed AA, Caldas C. Molecular classification and molecular forecasting of breast cancer: ready for clinical application. *J Clin Oncol* 2005;23:7350-60.
- West M, Blanchette C, Dressman H, et al. Predicting the clinical status of human breast cancer by using gene expression profiles. *Proc Natl Acad Sci U S A* 2001;98:11462-7.
- van 't Veer LJ, Dai H, van de Vijver MJ, et al. Gene expression profiling predicts clinical outcome of breast cancer. *Nature* 2002;415:530-6.
- Iwao-Koizumi K, Matoba R, Ueno N, et al. Prediction of docetaxel response in human breast cancer by gene expression profiling. *J Clin Oncol* 2005;23:422-31.
- Dressman HK, Hans C, Bild A, et al. Gene expression profiles of multiple breast cancer phenotypes and response to neoadjuvant chemotherapy. *Clin Cancer Res* 2006;12:819-26.
- Rouzier R, Perou CM, Symmans WF, et al. Breast cancer molecular subtypes respond differently to preoperative chemotherapy. *Clin Cancer Res* 2005;11:5678-85.
- Hess KR, Anderson K, Symmans WF, et al. Pharmacogenomic predictor of sensitivity to preoperative chemotherapy with paclitaxel and fluorouracil, doxorubicin, and cyclophosphamide in breast cancer. *J Clin Oncol* 2006;24:4236-44.
- Verbeek BS, Vroom TM, Adriaansen-Slot SS, et al. c-Src protein expression is increased in human breast cancer. An immunohistochemical and biochemical analysis. *J Pathol* 1996;180:383-8.
- Myoui A, Nishimura R, Williams PJ, et al. C-Src tyrosine kinase activity is associated with tumor colonization in bone and lung in an animal model of human breast cancer metastasis. *Cancer Res* 2003;63:5028-33.
- Susva M, Missbach M, Green J. Src inhibitors: drugs for the treatment of osteoporosis, cancer or both? *Trends Pharmacol Sci* 2000;21:489-95.
- Warmuth M, Damoiseaux R, Liu Y, Fabbro D, Gray N. SRC family kinases: potential targets for the treatment of human cancer and leukemia. *Curr Pharm Des* 2003;9:2043-59.
- Lombardo LJ, Lee FY, Chen P, et al. Discovery of *N*-(2-chloro-6-methyl-phenyl)-2-(6-(4-(2-hydroxyethyl)piperazin-1-yl)-2-methylpyrimidin-4-ylamino)thiazole-5-carboxamide (BMS-354825), a dual Src/Abl kinase inhibitor with potent antitumor activity in preclinical assays. *J Med Chem* 2004;47:6658-61.
- Nam S, Kim D, Cheng JQ, et al. Action of the Src family kinase inhibitor, dasatinib (BMS-354825), on human prostate cancer cells. *Cancer Res* 2005;65:9185-9.
- Johnson FM, Saigal B, Talpaz M, Donato NJ. Dasatinib (BMS-354825) tyrosine kinase inhibitor suppresses invasion and induces cell cycle arrest and apoptosis of head and neck squamous cell carcinoma and non-small cell lung cancer cells. *Clin Cancer Res* 2005;11:6924-32.
- Shah NP, Tran C, Lee FY, Chen P, Norris D, Sawyers CL. Overriding imatinib resistance with a novel abl kinase inhibitor. *Science* 2004;305:399-401.
- Doggrell SA. BMS-354825: a novel drug with potential for the treatment of imatinib-resistant chronic myeloid leukaemia. *Expert Opin Investig Drugs* 2005;14:89-91.
- Burgess MR, Skaggs BJ, Shah NP, Lee FY, Sawyers CL. Comparative analysis of two clinically active BCR-ABL kinase inhibitors reveals the role of conformation-specific binding in resistance. *Proc Natl Acad Sci U S A* 2005;102:3395-400.
- Talpaz M, Shah NP, Kantarjian H, et al. Dasatinib in imatinib-resistant Philadelphia chromosome-positive leukemias. *N Engl J Med* 2006;354:2531-41.
- Finn RS, Dering J, Wilson CA, et al. Biologic effects and identification of predictive markers of response to Dasatinib (BMS-354825), novel, oral, multi-targeted kinase inhibitor in human breast cancer cell lines *in vitro*. *Clin Cancer Res* 2005;11:9022s.
- Riss TL, Moravec RA. Comparison of MTT, XTT, and a novel tetrazolium compound for MTS for *in vitro* proliferation and chemosensitivity assays. *Mol Biol Cell* 1992;3:184a.
- Golub TR, Slonim DK, Tamayo P, et al. Molecular classification of cancer: class discovery and class prediction by gene expression monitoring. *Science* 1999;286:531-7.
- Staunton JE, Slonim DK, Coller HA, et al. Chemosensitivity prediction by transcriptional profiling. *Proc Natl Acad Sci U S A* 2001;98:10787-92.
- Pawitan Y, Bjöhle J, Amler L, et al. Gene expression profiling spares early breast cancer patients from adjuvant therapy—derived and validated in two population based cohorts. *Breast Cancer Res* 2005;7:R953-64.
- van de Rijn M, Perou CM, Tibshirani R, et al. Expression of cytokeratins 17 and 5 identifies a group of breast carcinomas with poor clinical outcome. *Am J Pathol* 2002;161:1991-6.
- Yamanashi Y, Fukushige SI, Semba K, et al. The yes-related cellular gene lyn encodes a possible tyrosine kinase similar to p56(lck). *Mol Cell Biol* 1987;7:237-43.
- Brown MT, Cooper JA. Regulation, substrates and functions of src. *Biochim Biophys Acta* 1996;1287:121-49.

33. Duxbury MS, Ito H, Ashley SW, Whang EE. CEACAM6 cross-linking induces caveolin-1-dependent, Src-mediated focal adhesion kinase phosphorylation in BxPC3 pancreatic adenocarcinoma cells. *J Biol Chem* 2004;279:23176–82.
34. Giancotti FG, Ruoslahti E. Integrin signaling. *Science* 1999;285:1028–32.
35. Thomas SM, Brugge JS. Cellular functions regulated by Src family kinases. *Annu Rev Cell Dev Biol* 1997;13:513–609.
36. Mao W, Irby R, Coppola D, et al. Activation of c-Src by receptor tyrosine kinases in human colon cancer cells with high metastatic potential. *Oncogene* 1997;15:3083–90.
37. Brsardi JS, Tice DA, Parson SJ. C-Src, receptor tyrosine kinases, and human cancer. *Adv Cancer Res* 1999;76:61–119.
38. Landen CN, Kinch MS, Sood AK. EphA2 as a target for ovarian cancer therapy. *Expert Opin Ther Targets* 2005;9:1179–87.
39. Bild AH, Yao G, Chang JT, et al. Oncogenic pathway signatures in human cancers as a guide to targeted therapies. *Nature* 2006;439:353–7.
40. Fan C, Oh DS, Wessels L, et al. Concordance among gene-expression-based predictors for breast cancer. *N Engl J Med* 2006;355:560–9.
41. Vekris A, Meynard D, Haaz MC, Bayssas M, Bonnet J, Robert J. Molecular determinants of the cytotoxicity of platinum compounds: the contribution of *in silico* research. *Cancer Res* 2004;64:356–62.
42. Peters D, Freund J, Robert L. Genome-wide transcriptional analysis of carboplatin response in chemosensitive and chemoresistant ovarian cancer cells. *Mol Cancer Ther* 2005;4:1605–16.
43. Roberts D, Schick J, Conway S, et al. Identification of genes associated with platinum drug sensitivity and resistance in human ovarian cancer cells. *Br J Cancer* 2005;92:1149–58.
44. Mariadason JM, Arango D, Shi Q, et al. Gene expression profiling-based prediction of response of colon carcinoma cells to 5-fluorouracil and camptothecin. *Cancer Res* 2003;63:8791–812.
45. Rouzier R, Rajan R, Wagner P, et al. Microtubule-associated protein  $\tau$ : a marker of paclitaxel sensitivity in breast cancer. *Proc Natl Acad Sci U S A* 2005;102:8315–20.
46. Jain A, Tindell CA, Laux I, et al. Epithelial membrane protein-1 is a biomarker of gefitinib resistance. *Proc Natl Acad Sci U S A* 2005;102:11858–63.
47. Elicieri BP, Paul R, Schwartzberg PL, et al. Selective requirement for Src kinases during VEGF-induced angiogenesis and vascular permeability. *Mol Cell* 1999;4:915–24.
48. Weis S, Cui J, Barnes L, Cheresh D. Endothelial barrier disruption by VEGF-mediated Src activity potentiates tumor cell extravasation and metastasis. *J Cell Biol* 2004;167:223–9.
49. Horne WC, Sanjay A, Bruzzaniti A, Baron R. The role(s) of Src kinase and Cbl proteins in the regulation of osteoclast differentiation and function. *Immunol Rev* 2005;208:106–25.